Molecular Imaging

DOI: 10.1002/ange.201209286

A R_{2p}/R_{1p} Ratiometric Procedure to Assess Matrix Metalloproteinase-2 Activity by Magnetic Resonance Imaging**

Valeria Catanzaro, Concetta V. Gringeri, Valeria Menchise, Sergio Padovan, Cinzia Boffa, Walter Dastrù, Linda Chaabane, Giuseppe Digilio, and Silvio Aime**

The approach to molecular imaging of enzymes by MRI typically relies upon imaging probes composed of an enzyme-cleavable moiety conjugated with a paramagnetic imaging reporter, such as a Gd^{III} chelate.[1] Upon enzymatic processing, the probe is transformed into a fragment with an altered relaxivity, leading to a different capability to enhance contrast in MR images with respect to the parent species. Ideally, the unprocessed (intact) form of the probe should be completely silent while the processed (cleaved) form should have a high relaxivity (that is, high contrast enhancement). In such a way the appearance of contrast within images can be unambiguously attributed to the result of enzymatic activity and not to dynamic changes of tissue probe concentration. However, gadolinium-based agents as enzyme responsive agents are never completely silent and both forms (unprocessed and processed) contribute to the overall contrast enhancement as a function of their respective relaxivities and tissue local concentrations.[2] Exact knowledge of the total concentration of Gd is essential to translate image contrast enhancement into the molar ratio of unprocessed versus processed forms, and thus into true enzyme activity maps. A viable solution to the concentration problem can be provided by the R_{2p}/R_{1p} ratiometric approach, which is based on the measurement of the ratio between the transverse and longitudinal paramagnetic contributions to the water proton relaxation rate; that is, R_{2p} and R_{1p} (with $R_i = 1/T_i$, $i = 1,2$). Although ratiometric approaches are well-established for CEST-MRI contrast agents,[2,3] there are only a couple of examples of application to Gd^{III} based relaxation agents, namely for pH and temperature imaging.[4,5]

Let us consider two Gd complexes, GdL and GdF, each characterized by its own transverse and longitudinal millimolar relaxivity (r_2 and r_1 terms respectively, in units of $mM^{-1}s^{-1}$). These species form the ratiometric pair, and the total paramagnetic relaxation enhancement of a mixture of the two can be expressed as:

$$R_{2p} = r_2^{GdL}\,[GdL] + r_2^{GdF}\,[GdF] \tag{1a}$$

$$R_{1p} = r_1^{GdL}\,[GdL] + r_1^{GdF}\,[GdF] \tag{1b}$$

where R_{ip} (s^{-1}) is the total paramagnetic relaxation enhancement (either transverse or longitudinal) and [GdL] and [GdF] are the concentrations of the two gadolinium species (mM). Equations (1a) and (1b) can be divided by the total concentration of gadolinium $C_T = [GdL] + [GdF]$, and combined to obtain (see the Supporting Information S1 for the derivation):

$$\frac{R_{2p}}{R_{1p}} = \frac{r_2^{GdF}}{r_1^{GdF}}\,\frac{1 + \left(\rho\,\frac{r_1^{GdL}}{r_1^{GdF}} - 1\right)\chi^{GdL}}{1 + \left(\frac{r_1^{GdL}}{r_1^{GdF}} - 1\right)\chi^{GdL}} \tag{2a}$$

$$\text{with } \rho = \frac{r_2^{GdL}}{r_1^{GdL}} \Big/ \frac{r_2^{GdF}}{r_1^{GdF}} \tag{2b}$$

Here, the R_{2p}/R_{1p} ratio is independent from the total concentration of Gd (C_T), whereas it only depends on χ^{GdL}, defined as the molar ratio of GdL over total gadolinium. Equation (2a) has the form of a rectangular hyperbola. The maximum variation of the R_{2p}/R_{1p} ratio, defined as $\Delta_{MAX} = (r_2^{GdL}/r_1^{GdL} - r_2^{GdF}/r_1^{GdF})$, increases with increasing the ratio of the ratios ρ, whereas the term r_1^{GdL}/r_1^{GdF} affects the shape of the curve (Eq. (2a) reduces to a straight line for $r_1^{GdL}/r_1^{GdF} = 1$; see Supporting Information S1 for simulations).

On the basis of these considerations, we have developed a new system for the ratiometric assessment of the activity of matrix metalloproteinases (MMPs), a family of extracellular matrix (ECM) endoproteases whose expression profile is strongly indicative of pathological conditions, including tumor and neurodegeneration.[6] Being MMP extracellular

[*] Dr. V. Catanzaro
Istituto di Ricerca Diagnostica e Nucleare SDN
Via Gianturco 113, 80143 Napoli (Italy)
Dr. C. V. Gringeri, Dr. G. Digilio
Department of Science and Technological Innovation, Università del Piemonte Orientale "A. Avogadro"
Viale T. Michel 11, 15121 Alessandria (Italy)
E-mail: giuseppe.digilio@mfn.unipmn.it
Dr. V. Menchise, Dr. S. Padovan
Institute for Biostructures and Bioimages (CNR) c/o Molecular Biotechnology Center
Via Nizza 52, 10125 Torino (Italy)
Dr. C. Boffa, Dr. W. Dastrù, Prof. S. Aime
Department of Chemisty & Center for Molecular Imaging, University of Turin
Via Nizza 52, 10125 Torino (Italy)
E-mail: silvio.aime@unito.it
Dr. L. Chaabane
Institute of Experimental Neurology (INSpe), Division of Neuroscience, San Raffaele Scientific Institute
Via Olgettina 58, 20132 Milan (Italy)

[**] This research was supported by funding from MEDITRANS (NMP4-CT-2006-026668), Regione Piemonte (Converging Technologies BIO-THER project; POR-FESR 2007-2013 "Piattaforme Innovative", PIIMDMT project) and MIUR PRIN 2010 no. 2010B5B2NL. C. Chirizzi and M. Capozza are acknowledged for technical assistance.

Supporting information for this article is available on the WWW under http://dx.doi.org/10.1002/anie.201209286.

© 2013 Wiley-VCH Verlag GmbH & Co. KGaA, Weinheim

enzymes, either secreted into the ECM or membrane bound ectoenzymes, they have been exploited as targets for molecular imaging of disease by several imaging modalities, including MRI.[7,8] We have synthesized a MMP-2 cleavable probe composed of the NIPVS*LYA sequence, inspired by previous work,[9] conjugated with a Gd-DOTA chelate at the N-terminus and with an alkyl chain at the C-terminus (Scheme 1). This amphiphilic probe has been inserted into the membrane of a DPPC/DSPE-PEG stealth liposome (see

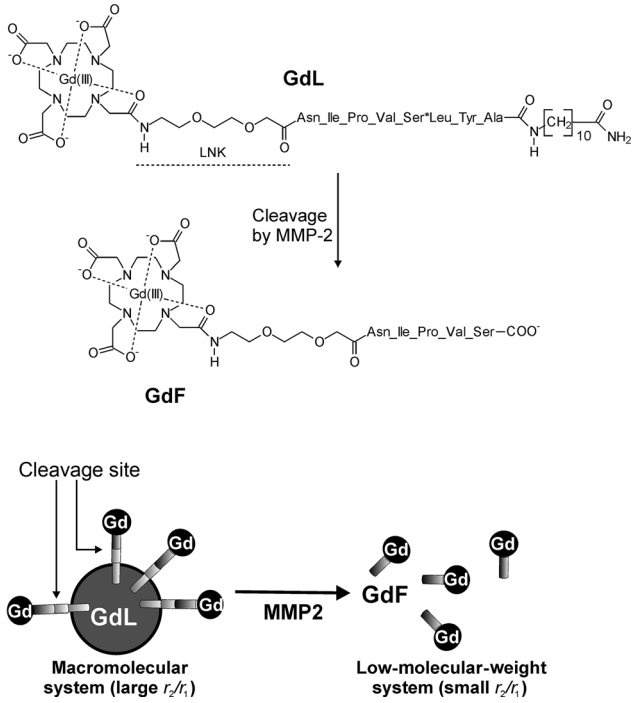

Scheme 1. Structure and representation of the ratiometric couple GdL/GdF.

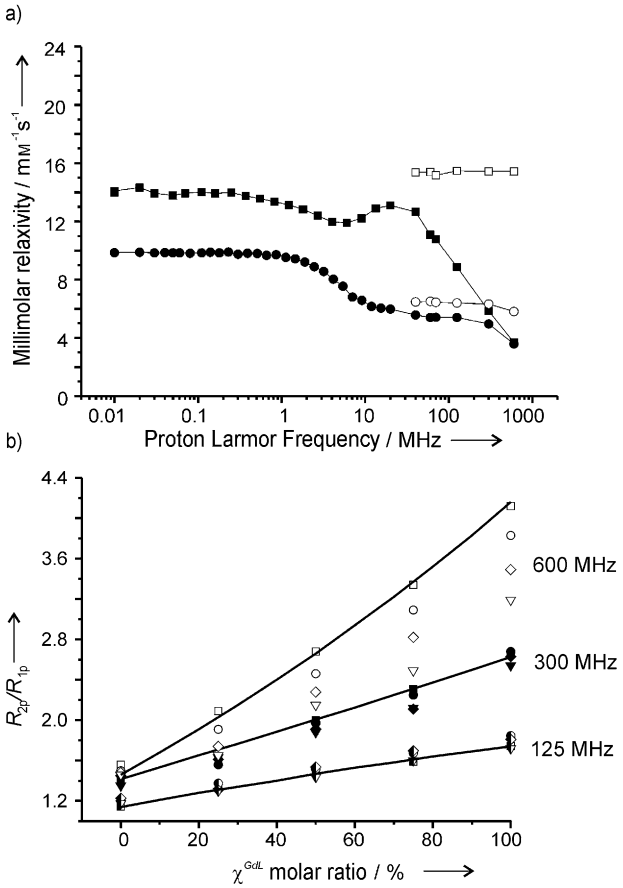

Figure 1. a) NMRD profiles (r_1 solid symbols; r_2 open symbols) of GdL (squares) and GdF (circles) at 25 °C, pH 7.2. b) R_{2p}/R_{1p} versus χ^{GdL} plots for mixtures of GdL/GdF measured at the indicated magnetic field (25 °C, pH 7.2). Solid lines are calculated from Equation (2) on the basis of the relaxivities of 1 mM solutions as shown in the NMRD profiles. Ratios were obtained from solutions at $C_T = 1$ mM (squares), 500 μM (circles), 250 μM (diamonds) and 125 μM (triangles).

the Supporting Information), to obtain a paramagnetic vesicle taking the role of species GdL of Equations (1) and (2). Liposome vesicles as carriers for MRI probes offer a number of advantages, including the possibility to achieve high relaxivities and to develop multimodal imaging probes.[10,11] The peptide sequence can be cleaved between Ser and Leu by MMP-2 with release of the soluble GdDOTA-lnk-NIPVS-COOH fragment, which then takes the role of GdF (Scheme 1).

The dependency of r_2 and r_1 with the magnetic field for the two members of the ratiometric pair (GdL and GdF) is reported as nuclear magnetic resonance dispersion (NMRD) profiles in Figure 1 a. As can be expected on theoretical grounds, the liposome GdL shows a smooth r_1^{GdL} relaxivity peak centered at 20–40 MHz followed by a steep dispersion to 3.7 $mM^{-1}s^{-1}$ (at 600 MHz). The relaxivity peak at 20–40 MHz is due to the so-called macromolecule effect, and it is characteristic of systems whose correlation time for molecular reorientation (τ_R) is slow, as it is the case of gadolinium compounds inserted into liposome membranes.[12] The NMRD peak is not as high as it would be expected on the basis of τ_R typical of liposomes because the rotational flexibility of the peptide chain makes local reorientation motions at the Gd center partly decoupled and faster than global reorientation, with a partial quenching of the macromolecule effect.[8,13] On the other hand, r_2^{GdL} remains approximately constant in the 20–600 MHz range, therefore the r_2^{GdL}/r_1^{GdL} ratio increases with increasing magnetic field. The GdF species (that is, the fragment that is released after MMP-dependent cleavage) presents NMRD features that are in line with those typical of Gd-DOTA-amide compounds of comparable size with a single r_1 dispersion. Importantly, the r_2^{GdF} relaxivity remains approximately constant in the whole range, but markedly lower than that of the GdL liposome counterpart.

Figure 1 a shows the experimentally measured R_{2p}/R_{1p} ratios for a series of samples prepared by mixing different amounts of GdL and GdF while keeping the total concentration of gadolinium fixed at 1 mM. These mixtures approximate a situation in which the GdL liposome is progressively transformed into GdF by MMP-2. As expected (Eq. (2), Figure 1 a), the sensitivity of R_{2p}/R_{1p} to χ^{GdL} increases with

 © 2013 Wiley-VCH Verlag GmbH & Co. KGaA, Weinheim

increasing magnetic field because of an increasing value of ρ. Figure 1b also shows the same measurements performed with serial dilutions, to ascertain whether R_{2p}/R_{1p} ratios were truly independent from the total Gd concentration C_T. At 600 MHz, R_{2p}/R_{1p} versus χ^{GdL} plots show a systematic deviation from the ideal behavior with decreasing values of C_T. This behavior is explained in terms of a subtle deviation from linearity of the R_{2p}^{GdL} versus [GdL] plot, introducing a residual dependency of R_{2p}/R_{1p} on the total Gd concentration (Eq. (1) no longer holds true). Such a detrimental effect is greatly attenuated at 300 MHz, where R_{2p}/R_{1p} ratios obtained within the C_T range 125–1000 μM are truly independent from C_T and responsive to χ^{GdL} with sensitivity $\Delta_{MAX} = 1.2$ (Figure 2). R_{2p}/R_{1p} is responsive to χ^{GdL} in a total Gd concentration independent manner down to 125 MHz, but the sensitivity becomes attenuated ($\Delta_{MAX} = 0.6$). Thus, the magnetic field of 300 MHz appears to be the best trade-off between sensitivity of R_{2p}/R_{1p} to χ^{GdL} and residual dependency of R_{2p}/R_{1p} on total Gd concentration. Therefore, this magnetic field has been selected to see whether our system was suitable to obtain R_{2p}/R_{1p} maps under a MRI setting. R_{1p} and R_{2p} maps of a phantom containing mixtures of GdL and GdF within the C_T range 125–1000 μM were acquired at 300 MHz and the corresponding R_{2p}/R_{1p} parametric image was constructed on a pixel-by-pixel basis (Figure 3a), while a plot of R_{2p}/R_{1p} with error bars as a function of ROI numbering is provided in Figure 3c. The contrast of the ratiometric map is independent from C_T and appears responsive only to χ^{GdL}, but the measurement uncertainty of R_{2p}/R_{1p} still shows a dependency on C_T. The uncertainty of R_{2p}/R_{1p} is contributed by errors propagating from the four quantities that are required to calculate the ratio (these quantities are R_1, R_2, $R_{1,dia}$, $R_{2,dia}$, where $R_{i,dia}$ are the baseline relaxation rates, R_i are the relaxation rates observed in the presence of gadolinium, and $R_{ip} = R_i - R_{i,dia}$). The uncertainty of R_{2p}/R_{1p} increases when R_{2p} and R_{1p} are small relative to the baseline relaxation rates $R_{2,dia}$ and $R_{1,dia}$; that is, when C_T approaches the detection limit (50 μM in buffer; see the Supporting Information). Although C_T does not formally affect the R_{2p}/R_{1p} ratio, it comes back into play by affecting the precision by which R_{2p}/R_{1p} (and thus χ^{GdL}) can be measured. Although the uncertainty of R_{2p}/R_{1p} increases with decreasing C_T, the difference of the R_{2p}/R_{1p} ratio at χ^{GdL} 100%, and 0% can still be appreciated at 125 μM. Large baseline relaxation rates (especially $R_{2,dia}$) can be found in tissue, leading to a negative impact on the sensitivity of the ratiometric method. To better mimic tissue baseline relaxation rates, a number of mixtures of GdL/GdF were dispersed within a 1% agar matrix and a ratiometric image was acquired (Figure 3b). As expected, the larger $R_{2,dia}$ of the agar matrix led to larger uncertainties of the R_{2p}/R_{1p} ratio (Figure 3c). However, the sensitivity of the R_{2p}/R_{1p} ratio to χ^{GdL} in agar was greatly enhanced compared to water ($\rho = 4.8$, $\Delta_{MAX} = 7.6$). Such a sensitivity enhancement is essentially

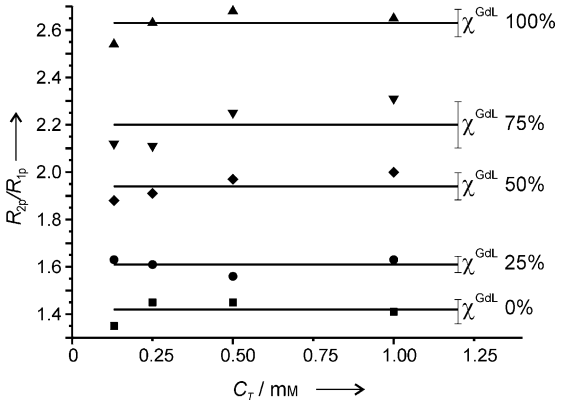

Figure 2. R_{2p}/R_{1p} ratios measured at 300 MHz as a function of C_T at five χ^{GdL} values: $\chi^{GdL} = 0$ (■); 25% (●); 50% (◆); 75% (▼), and 100% (▲). Straight lines represent each average ± SD.

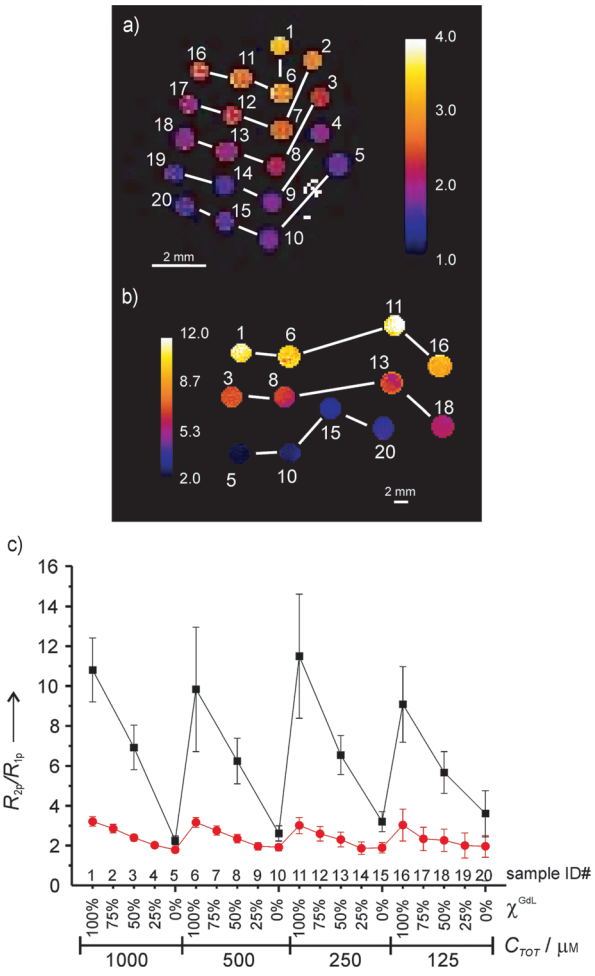

Figure 3. Pseudo-colored parametric R_{2p}/R_{1p} images obtained at 300 MHz (7 T). a) Water phantom containing an array of 20 mixtures of GdL/GdF with different molar ratios and different C_T (25 °C, pH 7.2). Total Gd concentrations: 1 mM (1 to 5), 500 μM (6 to 10), 250 μM (11 to 15), 125 μM (16 to 20). Within each of these series, χ^{GdL} is 100, 75, 50, 25, and 0% with increasing numbering order. Lines connect samples with the same χ^{GdL} but different C_T. b) 1% agar phantom containing an array of 12 mixtures GdL/GdF. Wells with the same numbering have the same composition. c) Plot of the R_{2p}/R_{1p} ratio as a function of well number. C_T and χ^{GdL} are given as label of the *x*-axis. ■ agar phantom, ● water phantom. Error bars represent ± one SD.

© 2013 Wiley-VCH Verlag GmbH & Co. KGaA, Weinheim

linked to the increase of r_2^{GdL} over r_1^{GdL}, r_2^{GdF} and r_1^{GdF} (Supporting Information, Table S1), because the high microviscosity of the agar matrix slows down the reorientation dynamics of the paramagnetic liposome. As a result, the sensitivity improvement makes up for the negative effects of large baseline $R_{2,dia}$, and the R_{2p}/R_{1p} ratio remains responsive to the GdL/GdF mixing ratio down to the detection limit (120 μM in 1% agar).

Finally we evaluated the feasibility of the ratiometric approach in kinetic experiments by incubating the MMP responsive GdL liposomes with MMP-2 and measuring the change of R_{2p} and R_{1p} as a function of the incubation time. The reaction, as far as followed by the change of R_{2p} with time (300 MHz, 25 °C), is first-order with respect to the substrate up to a substrate concentration of 1.0 mM, allowing for the calculation of $k_{cat}/K_m = 1.9 \times 10^4\ M^{-1} s^{-1}$. The peptide cleavage efficiency of the GdL system is smaller in respect to those reported for other sequences that have been used as MMP-responsive probes,[7] which is most likely because of steric hindrance stemming from the insertion of the MMP-2 substrate into the liposome membrane. Figure 4 shows the

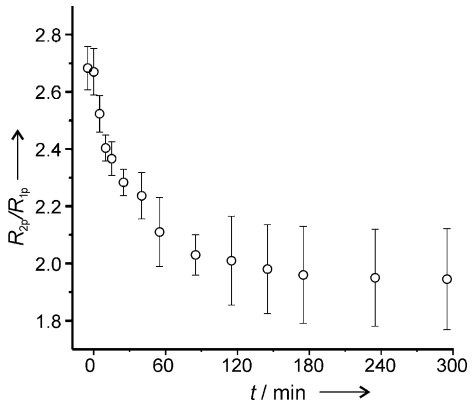

Figure 4. Plot of R_{2p}/R_{1p} versus time after incubation of the responsive liposome with MMP-2 (25 °C, pH 7.2, 300 MHz). Average ± SD are shown for ratios measured at C_T of 230, 450, and 900 μM.

change of R_{2p}/R_{1p} as a function of incubation time (each point in the graph is the average of kinetic experiments with an initial C_T of 230, 450, and 900 μM), showing a substantial independence of the change of R_{2p}/R_{1p} from C_T. A Δ_{MAX} of 0.65 is observed in this system, because only a fraction of GdL (for example, that protruding to the outer side of the liposome membrane) is recognized by MMP-2 and transformed into GdF, whereas Gd pointing to the inner liposome water cavity is not affected and introduces an offset contribution to the final observed relaxation rate.

In summary, we have presented a general ratiometric approach to obtain enzyme activity maps by MRI, and have exploited it to implement a novel liposome-based ratiometric couple to detect MMP-2 activity. The proposed method provides a means to evaluate the mixing ratio χ^{GdL} between the unprocessed (GdL) and the processed (GdF) form of a ratiometric pair. In principle this parameter can be directly related to the activity of MMP-2 in tissue. However, tissue influx/efflux rates of GdL and GdF are likely to be different, making the ratiometric χ^{GdL} dependent upon a function of both MMP activity and pharmacokinetics. To account for pharmacokinetic effects, an empirical calibration curve linking ratiometric χ^{GdL} measurements with histochemical/biochemical evaluations of MMP activity is required. Without a proper calibration, this method will not give a quantitative number of enzyme activity, but a relative estimate. The liposome-based MRI reporter is well amenable to combine imaging and therapy in an all-in-one system, eventually providing a theranostic approach to MMP-related pathologies, including cancer.[14]

Experimental Section

Compounds GdL and GdF were synthesized by solid-phase peptide synthesis essentially as described previously.[8] Liposomes were made by hydrating a thin film composed of DPPC/Methoxy-DSPE-PEG/GdL 66:9:25 w/w, and sonication to obtain vesicles with typical diameter of 80 ± 20 nm and polydispersity index of 0.2 as measured by DLS. MR images and relaxation rates measurements were carried out with Bruker MRI scanners operating at 125 MHz (3 T) and 300 MHz (7 T). For T_1 maps, a RARE-VTR sequence was used with RARE factor = 1, 16 TR values from 80 to 15000 ms, TE 10 ms, NEX 4, FOV = 2.6 × 2.6 cm, matrix 192 × 192 (spatial resolution 0.135 mm/pixel), slice thickness 2 mm. T_2-maps were obtained with a MSME sequence with 32 variable TE (10 to 320 ms), TR 15000 ms, NEX 4, FOV = 2.6 × 2.6 cm, matrix 192 × 192 (spatial resolution 0.135 mm/pixel), slice thickness 2 mm. More experimental details can be found the Supporting Information.

Received: November 20, 2012
Published online: February 28, 2013

Keywords: gadolinium · liposome · matrix metalloproteinases · molecular imaging · MRI probe

[1] a) S. Aime, M. Botta, E. Terreno, *Adv. Inorg. Chem.* **2005**, *57*, 197–237; b) A. Y. Louie, M. M. Huber, E. T. Ahrens, U. Rothbacher, R. Moats, R. E. Jacobs, S. E. Fraser, T. J. Meade, *Nat. Biotechnol.* **2000**, *18*, 321–325.

[2] a) M. Woods, D. E. Woessner, D. Sherry, *Chem. Soc. Rev.* **2006**, *35*, 500–511; b) D. L. Longo, W. Dastrù, G. Digilio, J. Keupp, S. Langereis, S. Lanzardo, S. Prestigio, O. Steinbach, E. Terreno, F. Uggeri, S. Aime, *Magn. Reson. Med.* **2010**, *65*, 202–211.

[3] T. Chauvin, P. Durand, M. Bernier, H. Meudal, B.-T. Doan, F. Noury, B. Badet, J.-C. Beloeil, E. Toth, *Angew. Chem.* **2008**, *120*, 4442–4444; *Angew. Chem. Int. Ed.* **2008**, *47*, 4370–4372.

[4] S. Aime, F. Fedeli, A. Sanino, E. Terreno, *J. Am. Chem. Soc.* **2006**, *128*, 11326–11327.

[5] E. Terreno, D. Delli Castelli, C. Cabella, W. Dastrù, A. Sanino, J. Stancanello, L. Tei, S. Aime, *Chem. Biodiversity* **2008**, *5*, 1901–1912.

[6] a) E. I. Deryugina, J. P. Quigley, *Cancer Metastasis Rev.* **2006**, *25*, 9–34; b) G. A. Rosenberg, *Lancet Neurol.* **2009**, *8*, 205–216.

[7] a) R. L. Scherer, J. O. McIntyre, L. M. Matrisian, *Cancer Metastasis Rev.* **2008**, *27*, 679–690; b) R. Lebel, B. Jastrzebska, H. Therriault, M. M. Cournoyer, J. O. McIntyre, E. Escher, W. Neugebauer, B. Paquette, M. Lepage, *Magn. Reson. Med.* **2008**, *60*, 1056–1065; c) E. S. Olson, T. Jiang, T. A. Aguilera, Q. T. Nguyend, L. G. Ellies, M. Scadeng, R. Y. Tsien, *Proc. Natl. Acad. Sci. USA* **2010**, *107*, 4311–4316; d) B. Jastrzebska, R. Lebel, H. Therriault, J. O. McIntyre, E. Escher, B. Guérin, B. Paquette,

 © 2013 Wiley-VCH Verlag GmbH & Co. KGaA, Weinheim

W. A. Neugebauer, M. Lepage, *J. Med. Chem.* **2009**, *52*, 1576 – 1581.
[8] C. V. Gringeri, V. Menchise, S. Rizzitelli, E. Cittadino, V. Catanzaro, G. Dati, L. Chaabane, G. Digilio, S. Aime, *Contrast Media Mol. Imaging* **2012**, *7*, 175 – 184.
[9] B. E. Turk, L. L. Huang, E. T. Piro, L. C. Cantley, *Nat. Biotechnol.* **2001**, *19*, 661 – 667.
[10] a) D. Delli Castelli, E. Gianolio, S. Geninatti Crich, E. Terreno, S. Aime, *Coord. Chem. Rev.* **2008**, *252*, 2424 – 2443; b) E. Terreno, C. Boffa, V. Menchise, F. Fedeli, C. Carrera, D. Delli Castelli, G. Digilio, S. Aime, *Chem. Commun.* **2011**, *47*, 4667 – 4669.
[11] W. J. M. Mulder, G. J. Strijkers, G. A. F. van Tilborg, A. W. Griffioen, K. Nicolay, *NMR Biomed.* **2006**, *19*, 142 – 164.
[12] M. Botta, L. Tei, *Eur. J. Inorg. Chem.* **2012**, 1945 – 1960.
[13] F. Kielar, L. Tei, E. Terreno, M. Botta, *J. Am. Chem. Soc.* **2010**, *132*, 7836 – 7837.
[14] C. Grange, S. Geninatti-Crich, G. Esposito, D. Alberti, L. Tei, B. Bussolati, S. Aime, G. Camussi, *Cancer Res.* **2010**, *70*, 2180 – 2190.

 © 2013 Wiley-VCH Verlag GmbH & Co. KGaA, Weinheim